J Sol-Gel Sci Technol (2013) 67:442–450
DOI 10.1007/s10971-013-3098-2

ORIGINAL PAPER

The preparation and characterization of photo-responsive sol–gel materials for 2,4-dichlorophenoxyacetic acid by surface imprinting

Cheng-Bin Gong · Yu-Zhu Yang · Chao Gao · Qian Tang · Cheuk-Fai Chow · Jing-Dong Peng · Michael Hon-Wah Lam

Received: 4 November 2012 / Accepted: 21 June 2013 / Published online: 29 June 2013

Abstract The primary objective of this work is to develop a photo-responsive surface molecularly imprinted polymer (SMIP) for 2,4-dichlorophenoxyacetic acid (2,4-D) to overcome the shortcomings of conventional molecularly imprinted polymers. A photo-responsive functional monomer was firstly prepared by covalent connecting azobenzene and 2,4-D. The photo-responsive SMIP was then prepared on SiO_2 nanoparticles via sol–gel process, and 2,4-D was removed via hydrolysis in acid. The SMIP shows specific affinity to 2,4-D and reversible uptake and release of 2,4-D upon alternate irradiation at 365 and 440 nm, respectively. The favorable binding strength of the imprinted receptor sites in the SMIP for 2,4-D is found to be $2.51 \times 10^4\ M^{-1}$. Density of receptor sites in the SMIP material is 10.59 μmol/g SMIP. The SMIP requires a shorter time to reach equilibrium than does the conventional molecularly imprinted polymer. The well-defined core-shell structure was clearly visualized by high resolution transmission electron microscopy.

Keywords Surface imprinting · 2,4-Dichlorophenoxyacetic acid · Sol–gel materials · Photo-responsive

1 Introduction

The development of new materials that are able to undergo significant change in their bulk properties upon specific external stimuli, such as temperature, pH, ionic and solvent compositions, concentration of specific chemical or biochemical species, electric field and light irradiation, is a hot research topic in the field of materials science [1, 2]. These classes of materials have potential applications in drug-delivery [3], bio-process technology [4], separation sciences [5], and chemical sensing [6]. Molecular imprinting is a template-directed polymerization/assembly process. With a suitable choice of functional monomers, molecularly imprinted polymers with a substrate affinity that can be switched by externally applied stimuli should be possible. For example, uptake and release of analytes have been photo-regulated using photo-responsive MIP [7–11]. Therefore, molecular imprinted polymers (MIPs) have already been applied to many different fields in chemistry, materials science and life sciences [12]. However, in conventional molecular imprinting, MIPs were generally synthesized by free radical polymerization, in which the rate of chain propagation cannot be controlled and polymers generally have a broad size distribution due to side reactions. Moreover, these MIPs often exhibit incomplete template removal, minimal binding capacity, slow mass transfer rate, and irregular material shapes [13].

Electronic supplementary material The online version of this article (doi:10.1007/s10971-013-3098-2) contains supplementary material, which is available to authorized users.

C.-B. Gong · Y.-Z. Yang · C. Gao · Q. Tang (✉) · J.-D. Peng
College of Chemistry and Chemical Engineering, Southwest University, Chongqing, China
e-mail: qiantang@swu.edu.cn

C.-B. Gong · Y.-Z. Yang · C. Gao · Q. Tang
The Key Laboratory of Applied Chemistry of Chongqing Municipality, Chongqing 400715, China

C.-F. Chow
Department of Science and Environmental Studies, The Hong Kong Institute of Education, Hong Kong, China

M. H.-W. Lam
Department of Biology and Chemistry, City University of Hong Kong, Hong Kong, China

Surface molecularly imprinted technique (SMIT) which controls templates to be situated at the surface or in the proximity of material surface was then developed to overcome those shortcomings of MIPs. Compared with traditional MIP, SMIP materials have significant advantages, such as fixing the binding sites maximally on the support surface, complete removal of templates, good accessibility to the target species, low mass-transfer resistance, enhanced recognition ability, as well as strengthened separation efficiency of target molecules [14]. Inorganic materials such as silica at micro- and nanometer scale is a best choice for the support due to their distinguished advantages, such as high physical and chemical stability, high degree of order or periodicity, and being functionalized in a straightforward manner.

2,4-Dichlorophenoxyacetic acid (2,4-D) is widely used as a plant growth regulator for agricultural and non-agricultural purposes. Due to its polarity, residues of 2,4-D in soil, ground water, and plants are of concern, because of its moderate toxicity to biological organisms. Consequently, monitoring of environmental levels of 2,4-D is an important goal for assessing the environmental impact of this chemical. Conventional methods for the analysis of 2,4-D are generally based on high-performance liquid chromatography (HPLC) [15, 16], gas chromatography (GC) [17], and mass-spectroscopy-coupled techniques (MSCT) [18], which require extensive sample pretreatments and preparation, including derivatization, and trained technical personnel. Recognition and sensing of 2,4-D using photo-responsive MIP or SMIP are simpler and faster. However, to the best of our knowledge, most of these works have been focused on MIP [19, 20], while the report on SMIP is scarce. In this study, we present a route to synthesize a photo-responsive surface molecularly imprinted polymer on SiO_2 nanoparticles for 2,4-D by introducing a photo-responsive functional azobenzene group into the functional monomer. As shown in Scheme 1, azobenzene and many of its derivatives can transform from the more stable *trans* form to the less stable *cis* form upon irradiation with UV, and can also transform from *cis* form to *trans* form upon irradiation with visible light or heat. Such photo-induced isomerization causes an obvious decrease in the distance between the para carbon atoms in azobenzene from about 9.0 Å in the *trans* form to 5.5 Å in the *cis* form [21]. The functional monomer also contains another function group which can interact with the template in *trans* form, and would release the template upon UV irradiation. The azobenzene group was then incorporated into the specific binding sites of SMIP during polymerization [7–9, 11, 22]. Such SMIP was expected to show complete template removal, maximum binding capacity, quick mass transfer rate, regular material shape and specific affinity to 2,4-D.

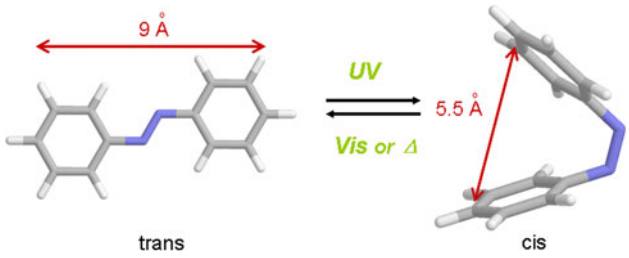

Scheme 1 Photoisomerization of azobenzene

2 Experimental

2.1 Materials and instruments

4-Nitrophenol (98 %), 2,4-dichlorophenoxyacetic acid (2,4-D), 2,4-dicholrophenyl-acetic acid (2,4-DA), 2,4-dichlorophenol (2,4-DCP), 3-chloropropyltriethoxysilane, thionyl chloride (99 %), tetraethoxysilane (TEOS) (98 %), KOH (99 %), KI (99 %), K_2CO_3, and triethylamine (TEA) were purchased from Aladdin Co. Shanghai, China. All solvents used were of analytical reagent grade in market sales.

^{1}H NMR and ^{13}C NMR (300 MHz) were performed on a Bruker AV–300 NMR instrument at ambient temperature using TMS as an internal standard. Elemental analysis was performed by a Leco CHN–900 micro carbon–hydrogen–nitrogen analyzer. Mass spectra were measured by a PE SCIEX API365 LC/MS/MS system. UV/Vis spectra was recorded with UV–4802 Spectrophotometer [UNICO (Shanghai) Instruments Co., Ltd.]. CEL–S500 Xe lamp (Beijing zhongjiao jinyuan keji Co., Ltd.) was used as a light source. 365 and 440 nm light were selected by 365 and 440 nm filter, respectively. HPLC were measured by Agilent 1100 liquid chromatography (Agilent Technologies, CA, USA). Fourier transform infrared spectra were recorded on a Perkin–Elmer Model GX Spectrometer using a KBr pellet method with polystyrene as a standard. The morphology of as synthesized SMIP was determined by a Philips CM200 FEG TEM.

2.2 Synthesis

The data of ^{1}H NMR, ^{13}C NMR, elemental analysis and MS are described in supporting information.

2.2.1 4,4′-Dihydroxyazobenzene (DiOH-AZO) and 3-iodopropyltriethanoxylsilane (IPTES)

DiOH-AZO was prepared according to Ref. [12]. Green solid. Yield 71.7 %, m.p. 220.1–221.3 °C (lit. 220 °C [23]). IPTES was prepared according to Ref. [20]. Colorless oil. Yield 82.3 %, b.p. 103–104 °C/1.2 kPa.

2.2.2 2,4-Dichlorophenoxyacetic chloride (DCPAC)

2,4-Dichlorophenoxyacetic acid (5.0 g, 22.0 mmol), thionyl ($SOCl_2$) (15.0 mL) and DMF (0.2 mL) were added in 50 mL two-necked flask. The resultant mixture was stirred for 3 h at *r. t.* and then heated to reflux for 5 h, followed by distillation under reduced pressure to remove excess $SOCl_2$. 4.8 g DCPAC in the form of pale yellow oil was obtained (yield 88.9 %) and was used in the following step without further purification.

2.2.3 2,4-Dichlorophenoxyacetyloxy-4′-hydroxylazobenzene (DCPA-AZO-OH)

DCPA-AZO-OH was synthesized according to a literature method with some modification [11]. It was found that bi-substituted product was overwhelmingly produced when K_2CO_3 was used. However, mono-substituted product could easily obtained by well controlled experimental conditions using a weaker base (triethanylamine) instead of K_2CO_3. The procedure was described as follows: 4,4′-dihydroxyazobenzene (1.1 g, 5.1 mmol) was dissolved in 50 mL dry acetone, the resultant dark mixture was cooled in an ice-bath and 0.5 g (4.9 mmol) triethylamine (TEA) was added. The 2,4-dichlorophenoxyacetic chloride (DCPAC) (1.4 g, 5.9 mmol) obtained in the previous step, dissolved in 10 mL dry acetone at 0 °C, was added dropwise to the mixture, and then stirred at *r. t.* for 24 h. Reaction progress was monitored by thin layer chromatography (TLC). Solvent was then removed under reduced pressure, and the residue was dissolved in 75 mL dichloromethane. Water (25 mL) was then added and the pH of the resultant solution was adjusted to 6 with diluted HCl. The aqueous layer was extracted with 10 mL dichloromethane; the organic extracts was washed with brine, dried over $MgSO_4$, and evaporated under reduced pressure. The crude product was purified by column chromatography on silica gel using 8:1 petroleum ether and ethyl acetate (v:v) as the eluents, and then recrystallized in dichloromethane and water (V/V = 2/1) to produce 1.3 g DCPA-AZO-OH as an orange solid. Yield 67.3 %.

2.2.4 2,4-Dicholrophenoxyacetyloxy-4′-[(triethanoxysilyl)propyloxy] azobenzene (DCPA-AZO-TESP) and 4-hydroxyl-4′-[(triethanoxysilyl)propyloxy] azobenzene (TESP-AZO-OH)

Under N_2 atmosphere, DCPA-AZO-OH (0.50 g, 1.2 mmol) and K_2CO_3 (0.17 g, 1.2 mmol) were induced in 50 mL four necked flask, and then 10 mL dry DMF was injected. The resultant red slurry was heated to 60 °C for about 90 min. The mixture was then cooled to room temperature and a solution of 3-iodopropyltriethanoxylsilane (2.0 g, 6.0 mmol) in 10 mL DMF was added dropwise. After the addition, the resultant clear red solution was heated to 75 °C for 5 h. Reaction progress was monitored by TLC until almost no DCPA-AZO-OH could be detected. The reaction mixture was cooled in an ice-bath, and then poured into 40 mL ice water containing 1.5 g sodium dihydrogen phosphate. The aqueous solution was extracted by 2 × 10 mL of ethyl acetate. The organic extracts were combined, washed with brine, dried over $MgSO_4$ and evaporated under reduced pressure to obtain crude product, which was purified by column chromatography on silica gel using 15:1 and 10:1 petroleum ether and ethyl acetate (v:v) as the eluents to afford 0.53 g DCPA-AZO-TESP as a red oil. Yield 71.1 %.

4-Hydroxyl-4′-[(triethanoxysilyl)propyloxy] azobenzene was synthesized in an identical fashion to DCPA-AZO-TESP, with the only difference being that DiOH-AZO (0.96 g, 4.5 mmol) was used in place of DCPA-AZO-OH. 0.65 g of red oil was obtained. Yield 34.7 %.

2.2.5 SMIP, SNIP and MIP

Silica microspheres were generally prepared according to the classical Stöber method [24]. It was found that silica in nanometer scale could be obtained by means of hydrolysis of alkyl silicates in distilled water (DI water) in the presensence of hydrazine hydrate instead of ammonia. The procedure was described as follows: 50 mL DI water, 5.0 mL TEOS and 0.30 mL of hydrazine hydrate were introduced into 100 mL flask. The mixture was stirred and heated to reflux for 10 h, and then cooled to *r. t.*, the resultant mixture was centrifuged, and the filter cake was washed with ethanol and distilled water and dried in reduced pressure to give 0.98 g SiO_2 as white powder.

Surface molecularly imprinted polymer was prepared as follows: 0.65 g (1.0 mmol) of DCPA-AZO-TESP and 0.70 mL (3.0 mmol) of tetraethoxylsilane (TEOS) were added dropwise to 30.0 mL *n*-butanol containing 0.40 g SiO_2, and then 0.30 mL distilled water and 0.60 mL $NH_3{\cdot}H_2O$ were added to the mixture under stirring. The resultant suspension was stirred at 30 °C for 14 h, the obtained mixture was centrifuged and washed with ethanol, acetone, DI water and a yellow powder was collected. The powder was suspended in 50 mL of 0.1 mol/L HCl and heated to reflux for 48 h to remove 2,4-D. The resultant residue was collected and washed with DI water till the pH of the filtrate was about 7.0. The resultant solid was dried in a freeze-dryer to afford yellow powder. The residual 2.4-D was removed by Soxhlet extraction with 200 mL methanol for 12 h to give 1.06 g of orange powder (SMIP).

The control surface imprinting material (SNIP) was prepared and treated in exactly the same way as the 2,4-D

surface imprinting sol–gel materials except that TESP-AZO-OH was used instead of DCPA-AZO-TESP in the polymerization procedure. Both materials were stored at room temperature in dark.

Molecular imprinted polymers was prepared in an identical fashion to SMIP, with the only difference being that no SiO_2 nanoparticles were added.

2.3 Spectroscopic characterization and photoisomerization studies

The procedure is similar to Ref. [25]. Monomer DCPA-AZO-TESP, TESP-AZO-OH and SMIP and SNIP were performed in acetonitrile (0.20 mg/mL) upon alternate irradiation at 365 and 440 nm, respectively. Suspensions of SMIP and SNIP were maintained with the help of a magnetic stirrer.

2.4 Binding kinetics

To investigate the adsorption dynamics of the SMIP, in each screw-capped vial, 3.0 mg SMIP and 1.0 mL of 5.0×10^{-5} mol/L 2,4-D were charged, the suspension was then sealed and agitated in the dark at 25 °C, and sampled at different intervals, the binding kinetics was tested by detecting the temporal evolution of 2,4-D concentration before and after adsorption in the solution. The concentration of free 2,4-D was measured by HPLC.

2.5 Rebinding assays

Binding properties of the imprinted material was studied by batch-type rebinding assays in acetonitrile in dark. The amount of analyte left after rebinding was determined by HPLC. Unless otherwise stated, all rebinding assays were performed with 3.0 mg sol–gel material in 1.0 mL acetonitrile at room temperature. In a typical rebinding experiment, known amount of 2,4-D was spiked into acetonitrile suspensions of SMIP in 2.0 mL screw-capped vials. These suspensions were then sealed and agitated for 14 h. Each of the suspensions was then filtered with microporous membrane. The HPLC was calibrated using standard solutions of 2,4-D of concentration ranging from 0 to 10^{-4} mol/L.

2.6 Selectivity studies

In order to estimate the selectivity of SMIP for 2,4-D, 2,4-DA and 2,4-DCP were used as competitive agents since their chemical molecular structures are similar to 2,4-D to a certain extent. 3.0 mg SMIP was dispersed in 1.0 mL of acetonitrile containing 1.0×10^{-5} mol/L of 2,4-D, 2,4-DA and 2,4-DCP, respectively. The mixture was shaken in dark at 25 °C for 14 h. The concentration of 2,4-D, 2,4-DA and 2,4-DCP were determined by HPLC after filtered with microporous membrane.

2.7 Photo-controlled uptake and release studies

In all experiments, suspension of SMIP (10.0 mg) in acetonitrile (3.0 mL) was used. All of the initial concentration of 2,4-D and 2,4-DA, 2,4-DCP were 5.0×10^{-5} mol/L. In a typical run, SMIP was transferred into the acetonitrile of the substrate in a quartz cell of 1.0 cm optical path-length fitted with a magnetic stirrer bar. The quartz cell was then screw-capped to ensure air-tightness and was placed in the sample holder. The suspension was stirred in dark for 14 h. For the photo-controlled release of 2,4-D, 2,4-DA and 2,4-DCP, the mixture was stirred and irradiated at 365 nm by the excitation beam from light source for 60 min. The stirring was then stopped and the mixture was allowed to settle for 3 min in darkness before 5.0 μL of the clear supernatant solution was taken out for HPLC analysis. Stirring and irradiation was resumed after the sampling of supernatant. Each round of irradiation was 60 min and substrate concentration in the solution and the UV–Vis absorbance change were measured at the end of each irradiation round. For the photo-controlled uptake of substrate, irradiation at 440 nm for 60 min was adopted. Besides this, all procedures were similar to those in the release experiments.

3 Results and discussion

3.1 Synthesis of SMIP

In order to prepare the template—functional monomer aggregate, 2,4-D chloride was synthesized and reacted with DiOH-AZO to form the corresponding ester. The silyl group was introduced onto the azobenzene chromophore via an ether linkage. The synthetic route of the SMIP is shown in Scheme 2.

The FT-IR spectra of the functional monomer (DCPA-AZO-TESP), SMIP (before and after the removal of the template (2,4-D) is shown in Fig. 1. Compared to the functional monomer (top line), the appearance of the characteristic absorption of 2,4-D ($\upsilon_{C=O}$ at 1,594 cm^{-1} and υ_{CH2} at 1,380 cm^{-1}) for SMIP (middle line) demonstrates that 2,4-D has been imprinted successfully into the as-prepared SMIP. After the removal of 2,4-D (bottom line), these characteristic absorption of 2,4-D disappeared, implying that the template, 2,4-D, has been removed completely from the SMIP material.

Scheme 2 The synthetic route for functional monomer and SMIP

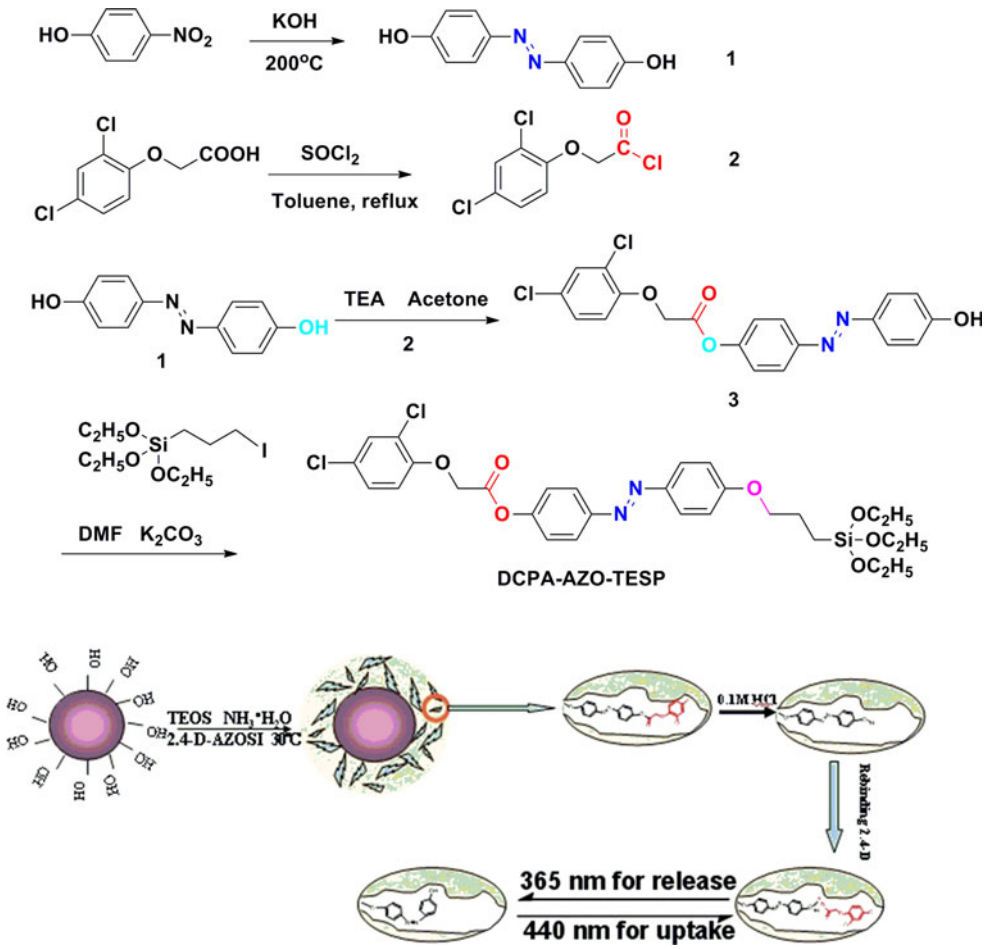

3.2 Characterization of SMIP

3.2.1 Photoisomerization properties of SMIP

The functional monomer, DCAP-AZO-TESP, shows good reversible photoisomerization properties (see supporting information S.Fig. 1 and S.Fig. 2) upon alternate irradiation at 365 and 440 nm. As expected, the initial UV/Vis spectrum indicates that DCAP-AZO-TESP is predominantly in its *trans*-configuration ($\lambda_{max} = 360$ nm, attributable to the π–π* transition). Upon irradiation at 365 nm, the drop of this *trans*-characteristic absorption band and the appearance of the absorption due to the *cis*-configuration ($\lambda_{max} = 450$ nm, attributable to the n–π* transition) was observed. And the photoisomerization process is good reversible, no obvious reduce of absorbance at 360 nm was observed after ten cycles.

Photoisomerization of the azobenzene chromophore in the SMIP materials was studied in acetonitrile by UV/Vis. Figure 2 shows the spectroscopic responses of SMIP material at *r. t.* after UV irradiation at 365 nm, followed by visible irradiation at 440 nm. It is found that irradiating SMIP at 365 nm causes the drop of the absorption peak at 360 nm (Fig. 2a). This is attributable to the *trans*- to *cis*- photo-isomerization of the azobenzene. The photo-stationary state was reached after 6 min of irradiation at 365 nm. Subsequent irradiation at 440 nm causes the reverse *cis*- to *trans*- photo-isomerization to take place (Fig. 2b). The rate constants for the *trans* → *cis* and *cis* → *trans* photoisomerization were measured to be $(1.19 \pm 0.04) \times 10^{-2}\ s^{-1}$ and $(4.16 \pm 0.17) \times 10^{-2}\ s^{-1}$, respectively, which was faster than the MIP (see supporting information S.Fig. 3), the reported organic–inorganic materials [11] and organic polymer materials [8, 9], demonstrating that SMIP possesses better specific affinity to target molecules due to more azobenzene chromophores fixed on the support surface.

Reversibility of the photo-isomerization of azobenzene chromophores in the SMIP material was studied by alternate irradiation at 365 and 440 nm (Fig. 3). No obvious reduce of absorbance at 360 nm was observed after eight cycles, demonstrating that the reversibility of the photo-isomerization of SMIP is robust.

3.2.2 The binding characteristics of SMIP

Binding kinetics of 2,4-D with the SMIP and conventional MIP were evaluated by batch adsorption experiments via incubationg a certain amount of the SMIP and conventional MIP in diluted 2,4-D solution. The binding kinetics were tested by detecting the temporal evolution of 2,4-D concentration before and after adsorption in the solution. Figure 4 illustrates the adsorption uptake of 2,4-D on the SMIP and conventional MIP versus the incubation time. It can be seen clearly that the SMIP requires a shorter time (60 min) to reach equilibrium than does the conventional MIP (80 min), indicating a quite faster binding process. This can be attributed to the existing of more effective binding sites on the SMIP surface, which allow the 2,4-D to diffuse into the SMIP pore rapidly during rebinding.

In order to examine the substrate specificity of the SMIP, the photo-regulated release and uptake of 2,4-DA, 2,4-DCP, whose structures are analogous to 2,4-D, by the surface imprinted material was studied. As shown in Fig. 5, the absorption efficiency of 2,4-D, 2,4-DA, 2,4-DCP were 34.3, 14.6 and 8.1 %, respectively after treated by SMIP. It can be seen clearly that the SMIP exhibits higher binding capacities towards 2,4-D than 2,4-DA and 2,4-DCP, demonstrating higher selectivity of the SMIP towards the template. The absorption efficiency of 2,4-D, 2,4-DA, 2,4-DCP for MIP was 26.7, 12.9 and 4.9 %, respectively. The improvement of imprinting efficiency for SMIP is attributable to the surface imprinting process.

The Scatchard analysis for SMIP was studied (Fig. 6). It was found that the Scatchard plot is a single straight line, which indicates the binding sites of SMIP are identical. The specific binding constant and the binding density are $2.51 \times 10^4\ M^{-1}$ and 10.59 μmol/g SMIP (for MIP, the binding density is 6.1 μmol/g MIP) respectively, which are 11 and 2.6 times larger than that of a conventional hybrid material [11], this denotes that SMIP has better specific affinity and larger binding capacity, because this "semi-covalent" surface imprinting technique possess the advantages of both covalent and non-covalent imprinting techniques, which utilizes covalent imprinting technique to assemble sites that bind the template in a non-covalent fashion on support surface.

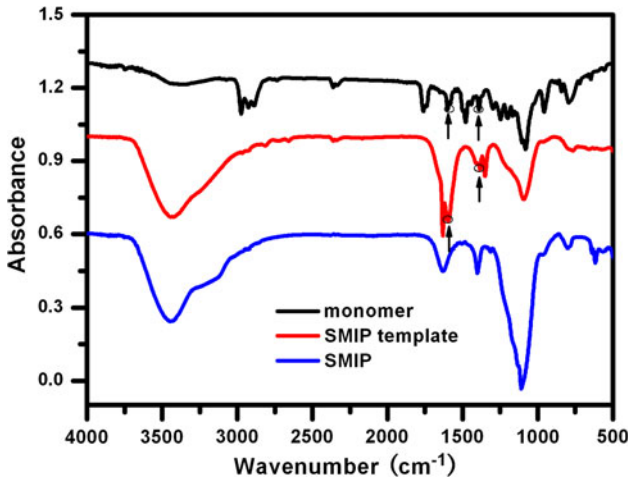

Fig. 1 FT-IR spectra of DCPA-AZO-TESP (functional monomer) and SMIP (before and after the removal of the template (2,4-D)

3.2.3 The photo-controlled release and uptake of 2,4-D with SMIP

It was found that the SNIP showed no photoregulated substrate release and uptake ability, except the binding of a small amount of 2,4-D bound at the initial stage of the experiment due to nonspecific binding, while SMIP

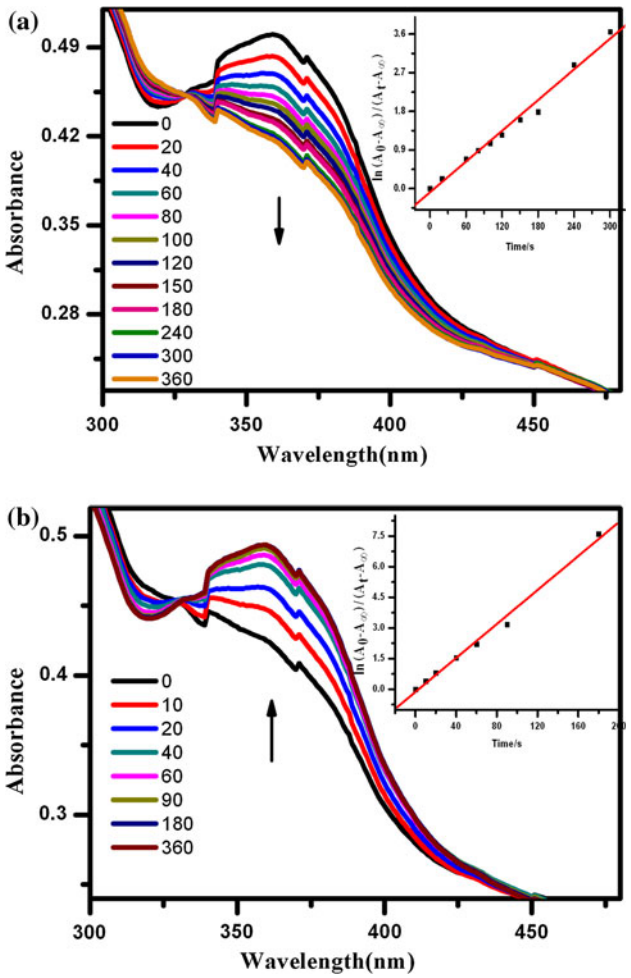

Fig. 2 Spectroscopic response of SMIP for 2,4-D (0.60 mg in 3.0 mL acetonitrile). **a** *trans* → *cis* photoisomerization upon irradiation at 365 nm; **b** *cis* → *trans* photoisomerization upon subsequent irradiation at 440 nm. Kinetics of the *trans* → *cis* photoisomerization is shown in the *inset*. Rate constants for the *trans* → *cis* and *cis* → *trans* photoisomerization are measured to be $(1.19 \pm 0.04) \times 10^{-2}\ s^{-1}$ and $(4.16 \pm 0.17) \times 10^{-2}\ s^{-1}$, respectively

showed good photoregulated substrate release and uptake ability. Figure 7 illustrates the change in the amount of imprinted receptors in the SMIP occupied by 2,4-D and its structural analogs, 2,4-DA, 2,4-DCP, in acetonitrile, upon alternate irradiation at 365 and 440 nm after subtraction of the nonspecific binding.

In the first cycle, 59.0 % of the imprinted receptors in the SMIP were filled by the substrate in the presence of excess 2,4-D in acetonitrile. Irradiation at 365 nm caused the release of 2,4-D from SMIP into acetonitrile. After the equilibrium state was reached, the fraction of bound receptors in the SMIP was reduced to 3.2 %. In other words, a total of 94.6 % of the receptor-bound substrate was released, which is larger than that obtained with a molecularly imprinted hydrogel [8] and a conventional MIP nanosphere [26]. It is noteworthy that the SMIP contains a solid SiO_2 core, which contains no binding sites for 2,4-D. In the second cycle, irradiation at 440 nm caused the fraction of occupied receptor sites to increase back to 56.3 %, demonstrating that 95.4 % of 2,4-D that had been previously released into acetonitrile has been uptaken again by SMIP. The fraction of bound receptors in the SMIP was reduced to 3.2 %, i.e., a total of 95.6 % of the receptor-bound substrate was released. In the third cycle, irradiation at 440 nm caused the fraction of occupied receptor sites to increase back to 59.3 %, which is nearly equivalent to the data obtain in the first cycle, and a total of 96.0 % of the receptor-bound substrate was released. This results proves that the photoregulated release and uptake of 2,4-D is repeatable. For the structural analogs of 2,4-D, although the imprinted SMIP was able to bring about some degree of photoregulated release and uptake, their extents were significantly smaller

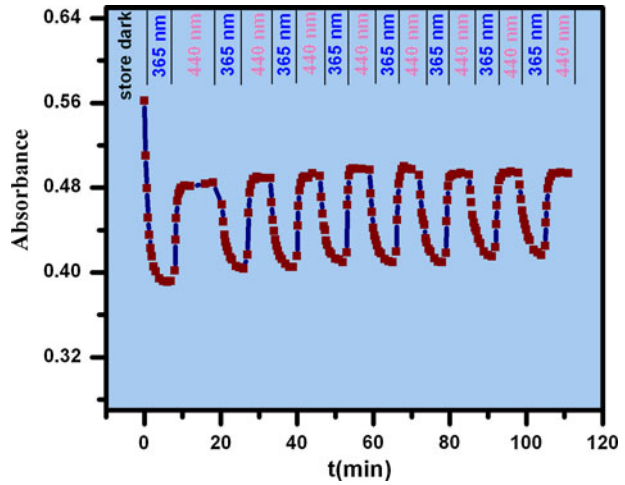

Fig. 3 Reversibility of the photoisomerization process of azobenzene chromophore in SMIP

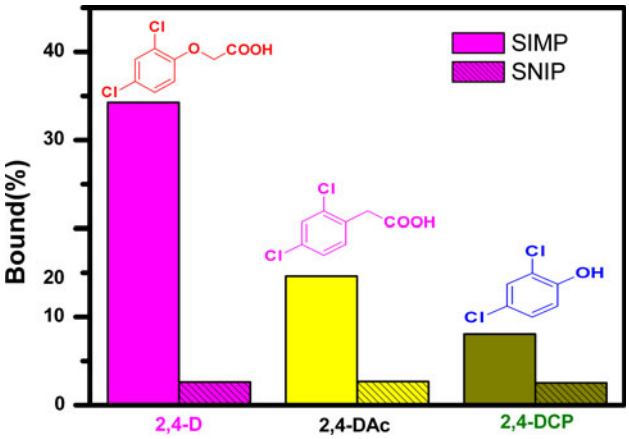

Fig. 5 Absorption efficiency of 2,4-D and its structural analog

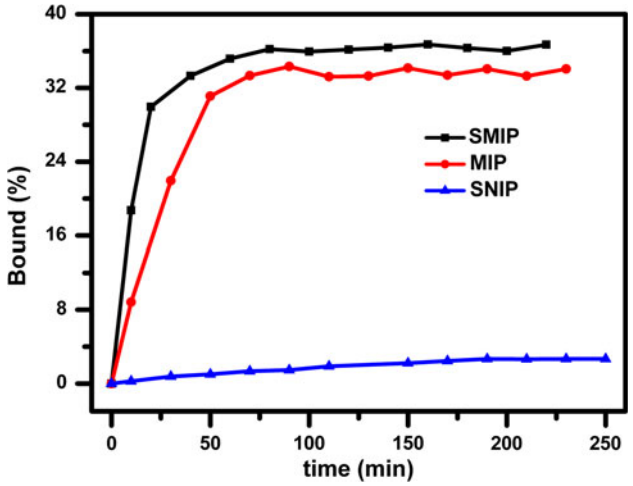

Fig. 4 Binding kinetics of 2,4-D on SMIP and MIP

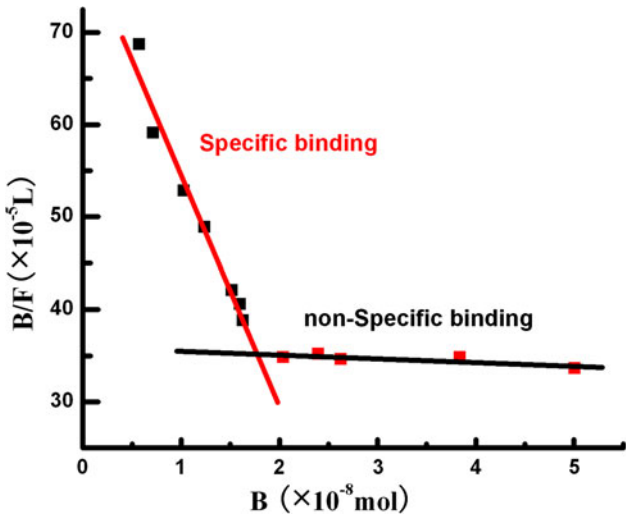

Fig. 6 Scatchard plot of the batch-type rebinding assay of SMIP with 2,4-D

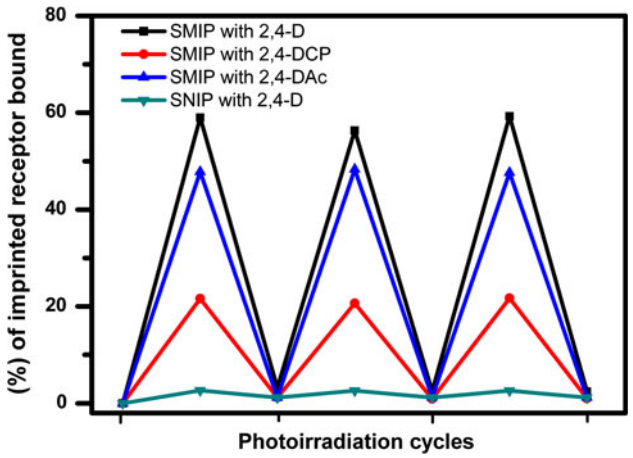

Fig. 7 Photocontrolled release and uptake of substrates by SMIP materials in acetonitrile. Nonspecific binding of substrate (revealed by parallel experiments on SNIP) has already been subtracted from the binding data

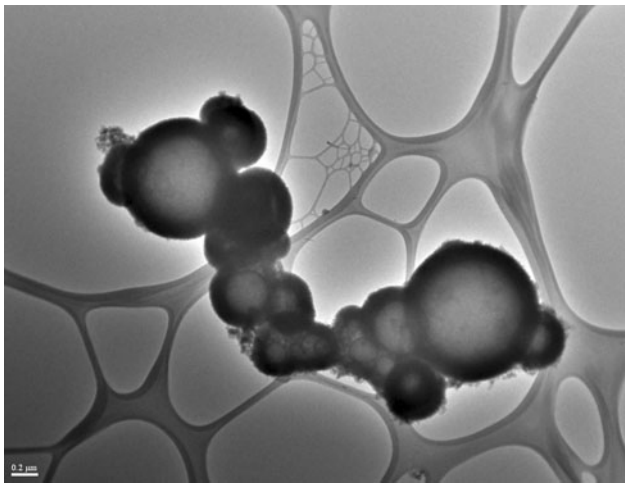

Fig. 8 HRTEM image of SMIP

than that of 2,4-D under similar experimental conditions. This demonstrates the substrate-specificity of the imprinted receptor sites in the SMIP for 2,4-D. The fraction of the imprinted receptors in the SMIP filled by 2,4-DA is larger than that by 2,4-DCP, this can be attributed to its chemical structure more similar to 2,4-D than 2,4-DCP.

3.2.4 The morphologies of SMIP

The morphology of the SMIP was observed by high resolution transmission electron microscopy (HRTEM) [27–29] (Fig. 8). The core-shell structure with well-defined shape and configuration was easily observed. It was found that the diameter of core is not uniform, while the surface

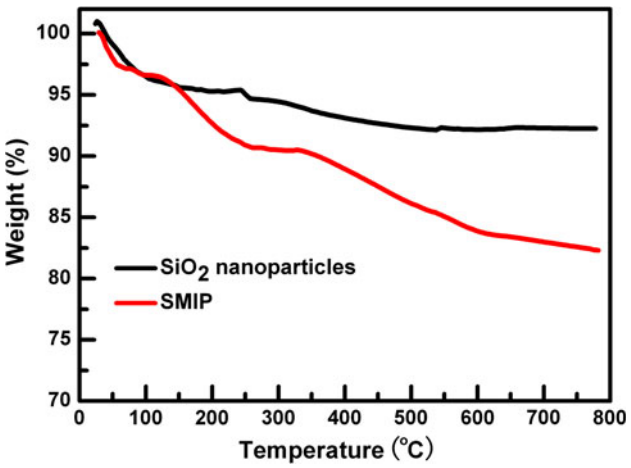

Fig. 9 The thermogravimetric *curves* of SiO_2 nanoparticles and SMIP

imprinting polymer shell is quite uniform and with an average thickness of ca. 50 nm.

3.2.5 Thermal gravimetric analysis (TGA)

The TG curves of SMIP and the silica are shown in Fig. 9. From the TGA curve of silica, the 5 % weight loss below 150 °C could be ascribed to the adsorbed water on silica surface, and the further 3 % weight loss was probably caused by the desorption of H_2O from Si–OH. From the TGA curve of SMIP, three weight loss processes were observed. Similarly, the 3.5 % weight loss below 100 °C could be ascribed to the adsorbed water, and the other 6.5 % weight loss between 100 and 300 °C was probably caused by desorption of H_2O from Si–OH. The further 7 % weight loss within the temperature range of 300–650 °C was caused by removal of the organic content in the surface imprinted layer, illustrating SMIP is more thermostable than conventional organic-based MIP.

4 Conclusions

A photo-responsive SMIP on SiO_2 nanoparticles with well-defined core-shell structure was developed by sol–gel process for the photo-controlled uptake and release of 2,4-D. Comparison with conventional MIP, the SMIP illustrates specific affinity to 2,4-D, quicker mass transfer rate, complete template removal as well as bigger binding capacity.

Acknowledgments The work described in this paper was supported by the National Natural Science Foundation of China (20872121), Croucher Chinese Visitorships 2012–2013, Research Funds for the Doctoral Program of Higher Education of China (20090182120010), Southwest University Doctoral Fund (SWUB2008075) and CQ CSTC 2013jcyjA50026.

References

1. Kumpfer JR, Rowan SJ (2011) Thermo-, photo-, and chemo-responsive shape-memory properties from photo-cross-linked metallo-supramolecular polymers. J Am Chem Soc 132: 12866–12874
2. Diaz DD, Kuhbeck D, Koopmans RJ (2011) Stimuli-responsive gels as reaction vessels and reusable catalysts. Chem Soc Rev 40:427–448
3. Aznar E, Marcos MD, Martinez–Manez R, Sancenon F, Soto J, Amoros P, Guillem C (2009) pH- and photo-switched release of guest molecules from mesoporous silica supports. J Am Chem Soc 131:6833–6843
4. Nandivada H, Ross AM, Lahann L (2010) Stimuli-responsive monolayers for biotechnology. Prog Polym Sci 35:141–154
5. Kanazawa H (2007) Thermally responsive chromatographic materials using functional polymers. J Sep Sci 30:1646–1656
6. Teng MJ, Kuang GC, Jia XR, Gao M, Li Y, Wei Y (2009) Glycine-glutamic-acid-based organogelators and their fluoride anion responsive properties. J Mater Chem 19:5648–5654
7. Tang Q, Gong CB, Lam MHW, Fu XK (2011) Preparation of a photoresponsive molecularly imprinted polymer containing fluorine-substituted azobenzene chromophores. Sens Actuators B Chem 156:100–107
8. Gong CB, Wong KL, Lam MHW (2008) Photoresponsive molecularly imprinted hydrogels for the photoregulated release and uptake of pharmaceuticals in the aqueous media. Chem Mater 20:1353–1358
9. Gong CB, Lam MHW, Yu HX (2006) The fabrication of a photoresponsive molecularly imprinted polymer for the photo-regulated uptake and release of caffeine. Adv Funct Mater 16:1759–1767
10. Jiang GS, Zhong SA, Chen L, Blakey I, Whitaker A (2011) Synthesis of molecularly imprinted organic-inorganic hybrid azobenzene materials by sol–gel for radiation induced selective recognition of 2,4-dichlorophenoxyacetic acid. Radiat Phys Chem 80:130–135
11. Tang Q, Gong CB, Lam MHW, Fu XK (2011) Photoregulated uptake and release of drug by an organic–inorganic hybrid sol–gel material. J Sol Gel Sci Technol 59:495–504
12. Shea KJ, Yan M, Roberts MJ (2002) Molecularly imprinted materials—sensors and other devices. Materials Research Society, Warrendale
13. He MQ, Song CC, Yan YS, Chen YQ, Wan JC (2011) Synthesis and recognition of molecularly imprinted polymers for gastrodin based on surface-modified silica nanoparticles. J Appl Polym Sci 121:2354–2360
14. Gao DM, Zhang ZP, Wu MH, Xie CG, Guan GJ, Wang DP (2007) A surface functional monomer-directing strategy for highly dense imprinting of TNT at surface of silica nanoparticles. J Am Chem Soc 129:7859–7866
15. Aulakh JS, Malik AK, Kaur V, Schmitt-Kopplin P (2005) A review on solid phase micro extraction-high performance liquid chromatography (SPME-HPLC) analysis of pesticides. Crit Rev Anal Chem 35:71–85
16. Fries E (2011) Determination of benzothiazole in untreated wastewater using polar-phase stir bar sorptive extraction and gas chromatography mass spectrometry. Anal Chim Acta 689:65–68
17. Lambropoulou DA, Albanis TA (2007) Methods of sample preparation for determination of pesticide residues in food matrices by chromatography-mass spectrometry-based techniques: a review. Anal Bioanal Chem 389:1663–1683
18. Gabaldon JA, Maquieira A, Puchades R (2007) Development of a simple extraction procedure for chlorpyrifos determination in food samples by immunoassay. Talanta 71:1001–1010
19. Yun YH, Shon HK, Yoon SD (2009) Preparation and characterization of molecularly imprinted polymers for the selective separation of 2,4-dichlorophenoxyacetic acid. J Mater Sci 44:6206–6211
20. Legido-Quigley C, Oxelbark J, De Lorenzi E, Zurutuza-Elorza A, Cormack PAG (2007) Chromatographic characterisation, under highly aqueous conditions, of a molecularly imprinted polymer binding the herbicide 2,4-dichlorophenoxyacetic acid. Anal Chim Acta 591:22–28
21. Kumar GS, Neckers DC (1989) Photochemistry of azobenzene-containing polymers. Chem Rev 89:1915–1925
22. Tang Q, Nie YT, Gong CB, Chow CF, Peng JD, Lam MHW (2012) Photo-responsive molecularly imprinted hydrogels for the detection of melamine in aqueous media. J Mater Chem 22:19812–19820
23. Babu RR, Kumaresan S, Vijayan N, Gunasekaran M, Gopalakrishnan R, Kannan P, Ramasamy P (2003) Growth of 4,4′-dihydroxyazobenzene (DHAB) and its characterization. J Cryst Growth 256:387–392
24. Stöber W, Fink A, Bohn E (1968) Controlled growth of monodisperse silica spheres in the micron size range. J Colloid Interface Sci 26:62–69
25. Tang Q, Meng XZ, Jiang HB, Zhou TY, Gong CB, Fu XK, Shi SQ (2010) Synthesis and characterization of photo- and pH-responsive nanoparticles containing amino-substituted azobenzene. J Mater Chem 20:9133–9139
26. Fang LJ, Chen SJ, Zhang Y, Zhang HQ (2011) Azobenzene-containing molecularly imprinted polymer microspheres with photoresponsive template binding properties. J Mater Chem 21:2320–2329
27. Peng Y, Xie Y, Luo J, Nie L, Chen Y, Chen LN, Du SH, Zhang ZP (2010) Molecularly imprinted polymer layer-coated silica nanoparticles toward dispersive solid-phase extraction of trace sulfonylurea herbicides from soil and crop samples. Anal Chim Acta 674:190–200
28. Wang S, Li Y, Wu XL, Ding MJ, Yuan LH, Wang RY, Wen TT, Zhang J, Chen LN, Zhou XM, Li F (2011) Construction of uniformly sized pseudo template imprinted polymers coupled with HPLC-UV for the selective extraction and determination of trace estrogens in chicken tissue samples. J Hazard Mater 186:1513–1519
29. Ma J, Yuan LH, Ding MJ, Wang S, Ren F, Zhang J, Du SH, Li F, Zhou XM (2011) The study of core-shell molecularly imprinted polymers of 17 beta-estradiol on the surface of silica nanoparticles. Biosens Bioelectron 26:2791–2795